Supplementary Information

A1. Contact line receding velocity of an evaporating drop

In colloidal drop drying processes, multi-ring depositions are formed due to the stick-slip motion of the contact line when it recedes as shown in Fig. 1. This stick-slip motion can be described as a step function in the drop radius, *R*, vs evaporation time, *t*, plot (Fig. A1b). However, it is difficult to quantify the contact line velocity during each stick-slip motion, due to the repetitive acceleration and deceleration nature of the processes. Instead, we assume the contact line undergoes a continuous motion during receding, as shown in the dashed line of Fig. A1b, in order to correlate the contact line velocity with *R*.

For an inkjet-printed pico-liter drop ($\mathrm{Bo} < 0.005$), where the effect of gravity can be neglected, the drop shape is considered as a spherical cap with contact angle θ and radius R shown in Fig. A1. When $t = t_0$, the volume of the drop can be written as

$$V(t_0) = \frac{1}{6}\pi R^3(t_0)\tan\frac{1}{2}\theta(t_0)[3+\tan^2\frac{1}{2}\theta(t_0)] \tag{A1}$$

On very hydrophilic substrates, the contact angle of the drop during receding approaches zero and it follows $\tan^2\left[\theta(t_0)/2\right] << 3$. Hence, the volume of the drop at $t = t_0$ can be simplified as

$$V(t_0) = \frac{1}{2}\pi R^3(t_0)\tan\frac{1}{2}\theta(t_0) \quad \text{for small } \theta \tag{A2}$$

Similarly, the volume of the drop at $t = t_0 + \delta t$ is given by

$$V(t_0+\delta t) = \frac{1}{2}\pi R^3(t_0+\delta t)\tan\frac{1}{2}\theta(t_0+\delta t) \quad \text{for small } \theta \tag{A3}$$

Utilizing Eqs. (A2) and (A3), it follows

$$\frac{dV(t_0)}{dt}=\lim_{\delta t\to 0}\frac{V(t_0+\delta t)-V(t_0)}{\delta t}=\frac{1}{2}\pi[\frac{\frac{d\theta(t_0)}{dt}}{2\cos^2\frac{1}{2}\theta(t_0)}R^3(t_0)+3R^2(t_0)\frac{dR(t_0)}{dt}\tan\frac{1}{2}\theta(t_0)] \quad \text{(A4)}$$

For an incompressible drop, $dm=\rho dV$, where m and ρ are mass and density of a drop. Hence, the drop contact line velocity at $t=t_0$ is given by reorganizing Eq. (A4)

$$\frac{dR}{dt}=\frac{1}{3R^2\tan\frac{1}{2}\theta}(\frac{2}{\rho\pi}\frac{dm}{dt}-\frac{0.5\frac{d\theta}{dt}}{\cos\frac{1}{2}\theta}R^3) \quad \text{(A5)}$$

For a very hydrophilic substrate, where the equilibrium contact angle of the drop is very small, the contact angle variation during drop receding is considered to be small, i.e., $\frac{d\theta}{dt}\sim 0$, which follows

$$\frac{dR}{dt}=\frac{2}{3\rho\pi R^2\tan\frac{1}{2}\theta}\left(\frac{dm}{dt}\right) \quad \text{(A6)}$$

The volume variation of the drop due to solvent evaporation, dm/dt, can be obtained by integrating the diffusion driven evaporation along the drop surface to yield[1]

$$\frac{dm}{dt}=-1.3\pi RD(1-\mathrm{RH})c_v \quad \text{(A7)}$$

where D is the diffusivity of water vapor in air, RH is the ambient relative humidity, and c_v is the saturated vapor concentration of the solvent.

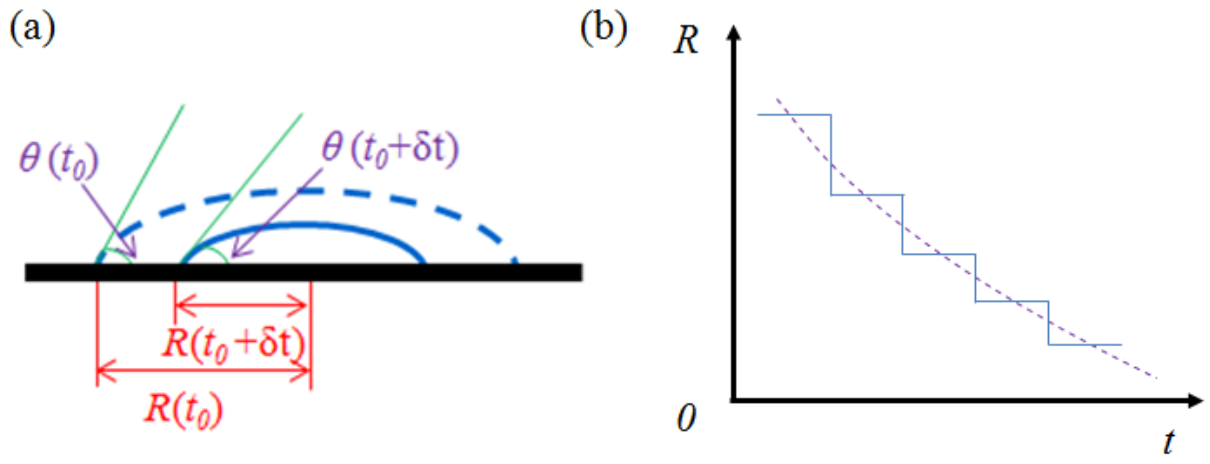

Figure A1: (a) Schematic illustration of a drop receding on a hydrophilic substrate. (b) Schematic step function of stick-slip motion of the contact line (solid lines) and the fitted linear curve (dash line) during drop receding. The dash line follows $R \sim \sqrt{t}$ by integrating Eq. (A9).

Substituting Eq. (A7) into Eq. (A6), the instantaneous contact line velocity is given by

$$U_{\mathrm{CL}} = \frac{dR}{dt} = -\frac{1.3 c_v D(1-\mathrm{RH})}{3\rho_l \tan\frac{1}{2}\theta}\frac{1}{R} \tag{A8}$$

Because the change in contact angle is trivial during drop receding on a very hydrophilic substrate, $\tan\left[\theta(t)/2\right]$ can be approximated as a constant and hence the contact line velocity inside a drying drop gives

$$U_{\mathrm{CL}} \sim 1/R \tag{A9}$$

which implies that the contact line velocity keeps increasing during drop receding.

A2. Particle deposition rate at contact line

Based on Eq. (A7), the volumetric solvent evaporation rate of the entire drop is

$$\frac{dV}{dt} = -\frac{1.3\pi RD(1-\mathrm{RH})c_v}{\rho_l} \tag{A10}$$

Because particles are accumulated and deposited along the drop edge, the volumetric particle deposition rate along the contact line gives $2\pi RndU_\mathrm{p}$ or $C_\mathrm{p}\left(dV/dt\right)/\left(1-\varepsilon\right)$, where d is the particle diameter, C_p the particle volume fraction, ε the deposition porosity, and n the number of layers of particles in the deposition. The radial growth rate of particle deposition, U_p, can hence be given by

$$U_\mathrm{p} = -\frac{1.3D(1-\mathrm{RH})c_v}{2dn\rho_l(1-\varepsilon)}C_\mathrm{p} \tag{A11}$$

Experimental evidence shows that the particle concentration in the central region of the drop does not change during drying[2]. Here, we assume that the particle concentration, layer of the particles, and porosity in the deposition do not change during evaporation, and hence the radial growth rate of particle deposition, U_p, is a constant during drop receding and is independent of the contact line radius, R, following

$$U_\mathrm{p} \sim const \tag{A12}$$

A3. Ring spacing of the multi-ring structure

During drop receding, when the contact angle decreases below a critical value, the depinning forces surpass the pinning forces driving the contact line to depin from the original location (R, θ) and slip to a new location ($R-\delta R$, $\theta+\delta\theta$), where the contact line pins again and forms a new ring at $R-\delta R$, as shown in Fig A2. Here, δR is the ring spacing at location R.

Assuming the drop is of spherical-cap shape both before and after slip and solvent evaporation is minimal during slip[3], the volume of the drop can be written as

$$V = \frac{1}{2}\pi R^3 \tan\frac{1}{2}\theta \tag{A13}$$

or

$$V = \frac{1}{2}\pi (R-\delta R)^3 \tan\frac{1}{2}(\theta+\delta\theta) \tag{A14}$$

Hence, the ring spacing, δR, can be expressed as a function of the instantaneous drop radius, R, as

$$\delta R = CR \tag{A15}$$

where $C = (1-\sqrt[3]{\dfrac{\tan\frac{1}{2}\theta - \tan^2\frac{1}{2}\theta\cdot\tan\frac{1}{2}\delta\theta - \tan^3\frac{1}{2}\theta}{\tan\frac{1}{2}\delta\theta + \tan\frac{1}{2}\theta}})$. Assuming θ and $\theta+\delta\theta$ keep constant at different ring positions[3-5], the coefficient C becomes a constant during drop evaporation. Hence, it follows

$$\delta R \sim R \tag{A16}$$

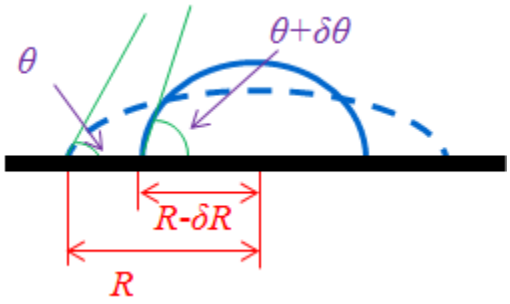

Figure A2: Schematic illustration of the stick-slip motion of the contact line.

A4. Scanning Electron Microscopy (SEM) images of deposition morphologies for colloidal drops with different particle loadings

Deposition morphologies of evaporating colloidal drops dried at 40% relative humidity with 20nm particles at particle loadings of 0.5%, 0.25%, and 0.1% are shown in Figs. A3, A4, and A5, respectively.

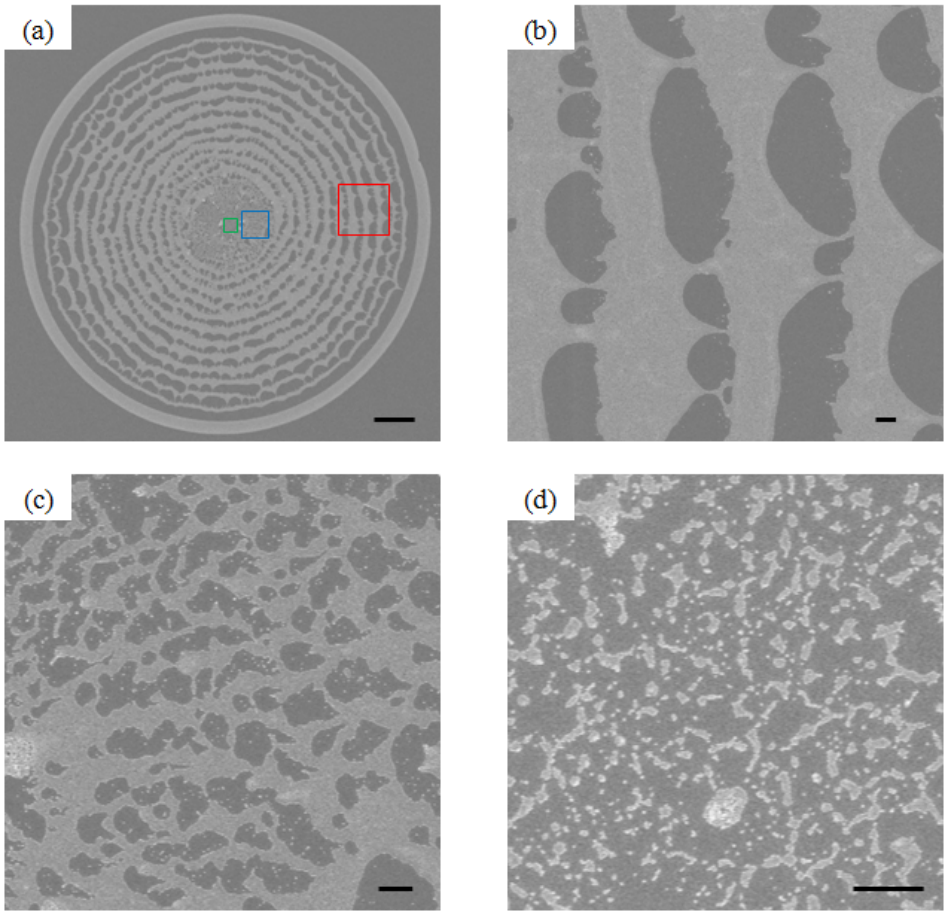

Figure A3: Deposition morphologies inside colloidal drops dried at 40% relative humidity with 20 nm particles at 0.5 % particle loading. (a) Overview morphology, (b) – (d) high magnification SEM images of: (b) the multi-ring in red box, (c) the foam in blue box, (d) the island in green box. The scale bars are 20 μm in (a) and 1 μm in (b) – (d).

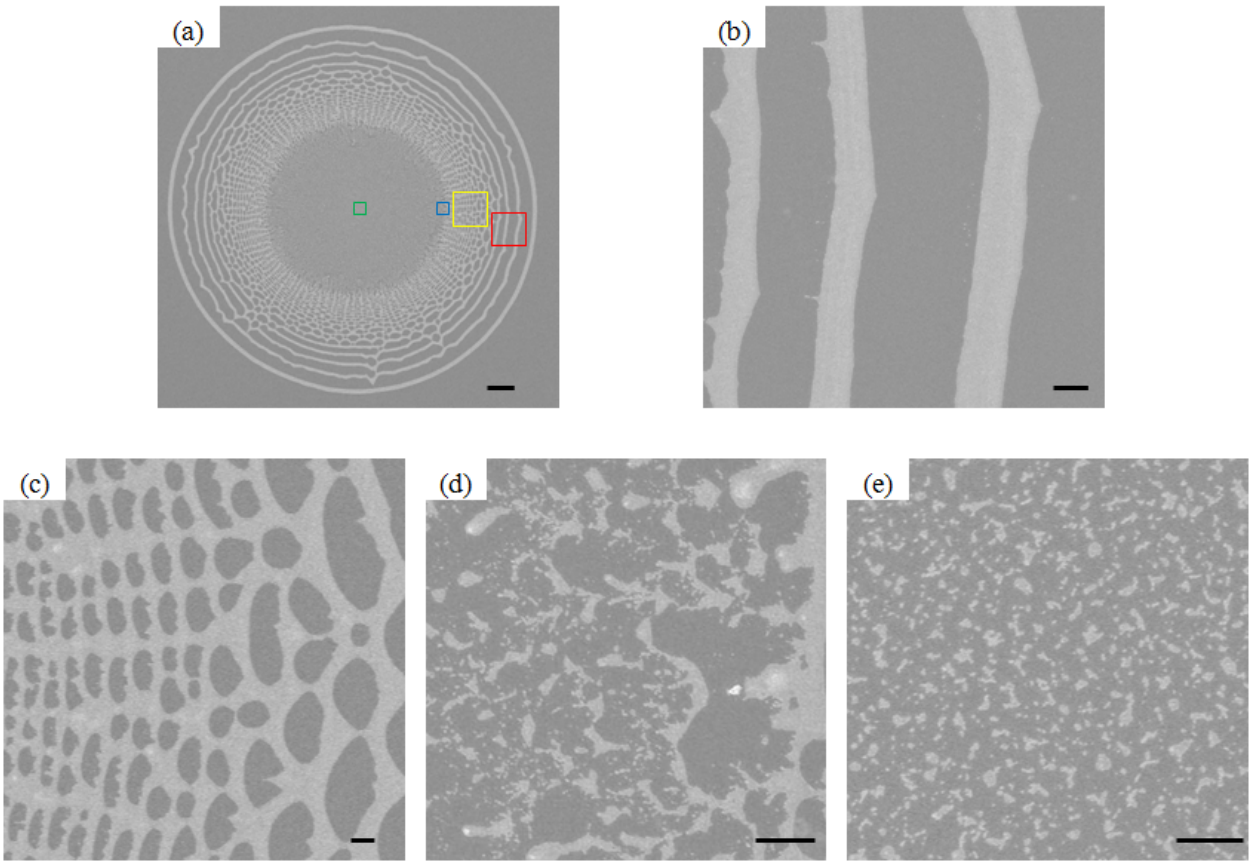

Figure A4: Deposition morphologies inside colloidal drops dried at 40% relative humidity with 20 nm particles at 0.25 % particle loading. (a) Overview morphology, (b) – (e) high magnification SEM images of: (b) the multi-ring in red box, (c) the spider web in yellow box, (d) the foam in blue box, (e) the island in the green box. The scale bars are 20 µm in (a) and 2 µm in (b) – (e).

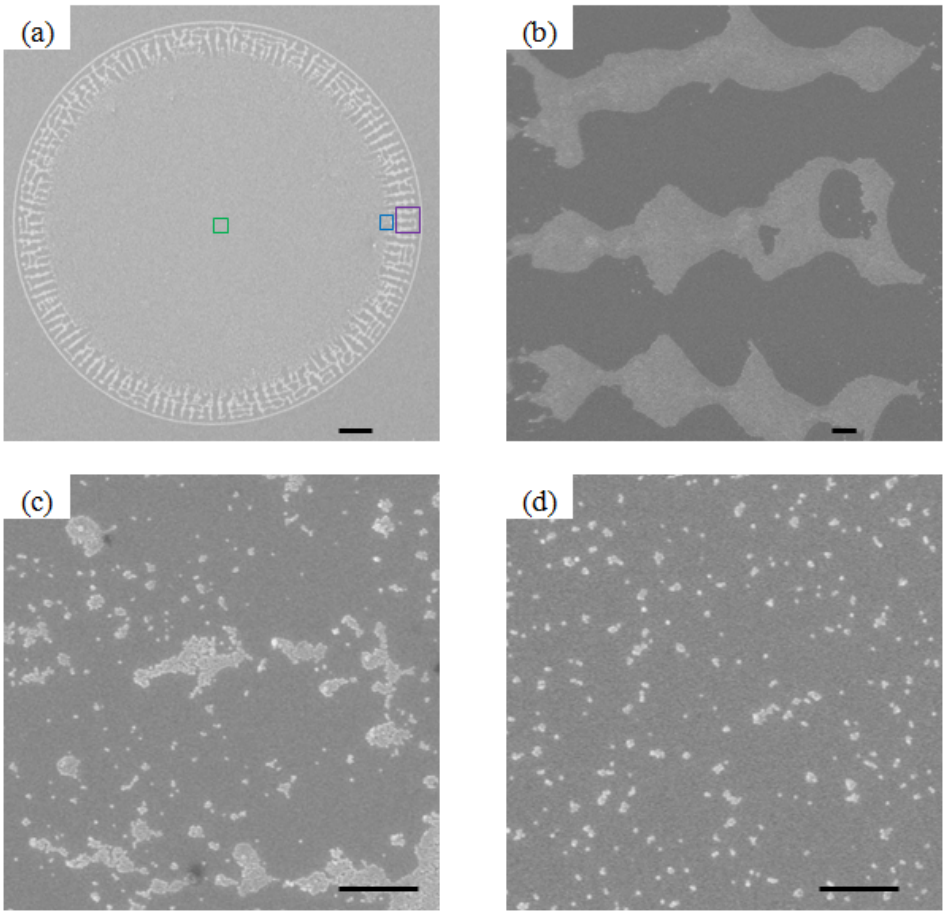

Figure A5: Deposition morphologies inside colloidal drops dried at 40% relative humidity with 20 nm particles at 0.1 % particle loading. (a) Overview morphology, (b) – (d) high magnification SEM images of: (b) the spoke in purple box, (c) the foam in blue box, (d) the island in the green box. The scale bars are 20 μm in (a) and 1 μm in (b) – (e).

REFERENCE

1. Hu, H.; Larson, R. G., Evaporation of a sessile droplet on a substrate. *Journal of Physical Chemistry B* **2002,** 106, (6), 1334-1344.

2. Kajiya, T.; Kaneko, D.; Doi, M., Dynamical Visualization of "Coffee Stain Phenomenon" in Droplets of Polymer Solution via Fluorescent Microscopy. *Langmuir* **2008,** 24, (21), 12369-12374.

3. Xu, J.; Xia, J. F.; Hong, S. W.; Lin, Z. Q.; Qiu, F.; Yang, Y. L., Self-assembly of gradient concentric rings via solvent evaporation from a capillary bridge. *Physical Review Letters* **2006,** 96, (6).

4. Tadmor, R., Line energy, line tension and drop size. *Surface Science* **2008,** 602, (14), L108-L111.

5. Maheshwari, S.; Zhang, L.; Zhu, Y. X.; Chang, H. C., Coupling between precipitation and contact-line dynamics: Multiring stains and stick-slip motion. *Physical Review Letters* **2008,** 100, (4).